

PREDICTING TRANSITION ON LOW-PRESSURE TURBINE PROFILES

Vincent Marciniak*, Edmund Kügeler* and Matthias Franke†

*German Aerospace Center – Institute of Propulsion Technology,
51147 Cologne, Germany
e-mail: vincent.marciniak@dlr.de, edmund.kuegeler@dlr.de

†MTU Aero Engines GmbH
Dachauer Str. 655
80995 Munich, Germany
e-mail: matthias.franke@muc.mtu.de

Key words: Computational Fluid Dynamics, Turbomachinery, Transition Modelling

Abstract. *In turbomachines, transitional flows are likely to occur over many components. In the case of a low-pressure turbine, the transition from laminar to turbulent boundary layer is often separation-induced. The overall blade losses depend among others physical effects on the size and the length of the separation bubble. The characteristics of the separation bubble are strongly linked with the Reynolds number and the turbulence intensity of the flow. So, turbomachinery designers require tools which could be used to achieve an accurate prediction of the laminar-turbulent transition. Many computational techniques are available to predict transitional behavior. However, only the computation of the Reynolds Averaged Navier-Stokes (RANS) equations seems to be able to be used in an industrial context, due to the relatively low computational resource required.*

The aim of this paper is to present and compare different approaches used to predict transition on practical test cases. Two models using experimental correlations to simulate transitional flows are described. The first uses boundary layer integral values, and the second uses only local values. The chosen test cases are two low-pressure turbine cascades with different aerodynamic loads and a multistage low-pressure turbine.

1 INTRODUCTION

For fifty years, the air traffic has increased steadily. The reduction of fuel consumption has become a very important objective in the design of aero-engines. For long range missions, the original turbojet engine has been replaced by the turbofan engine. Unfortunately, the different components of those engines require different rotational speeds and all the components need to work at a high efficiency level. A way to fulfill those requirements is the multi-spool arrangement. Depending on their roles, the fan and compressor stages are driven by different turbine stages. For instance, a fan which has a large radius will be driven by a low pressure turbine at the same low rotational speed.

In typical operating conditions, the flow over a low-pressure turbine is characterized by a relatively low Reynolds number. Initially laminar, the boundary layer developing over the blade may become turbulent. A turbulent boundary layer produces much more losses than a laminar one. This transition process is influenced by physical parameters of the flow such as the free stream turbulent intensity, the pressure gradient or the roughness of the blade¹

Depending on the combination of those parameters, different transition modes may be favored. Even if all the physical mechanism governing the transition modes are not well understood, the transition modes have been experimentally studied and classified². In a flow over typical turbomachine component, three types of transition mode are more likely to occur:

- Natural and Bypass Transition: At low turbulence intensity value, inside a laminar boundary layer instabilities will develop. Those disturbances will grow and eventually result in structures named Tollmien-Schlichting waves. Those waves can be amplified to end up in the formation of turbulent spots. The turbulent spots can finally merge to obtain a fully turbulent boundary layer. This is called the natural transition mode. For higher values of the free stream turbulent intensity, the process of amplification of disturbance can be accelerated or bypassed: this is called the bypass transition mode³.
- Separation-Induced Transition: Exposed to the effect of a strong enough adverse pressure gradient, a laminar boundary layer may separate from the wall. The contact of this separated layer with the free stream may favor a Kelvin-Helmholtz instability. This instability promotes a quick transition, and the flow, now turbulent reattaches. This is commonly denoted as a separation bubble⁴.
- Wake-Induced Transition: In the case of a multistage component, periodical wakes interact with the boundary layers. The wakes generated by upstream rows have a major influence over the transition of a downstream blade. The incoming wake has a quite high turbulent intensity (typical values between 15 and 20 percent) and can then promote a quick transition when penetrating a laminar boundary layer.

Concerning a low-pressure turbine profile, it should be emphasized that the adverse pressure gradient over the suction side of the blade promotes especially a separation-induced transition.

With the current design trend aiming to reduce the number of airfoils per row for the same performance⁵, High Lift (HL) and even Ultra High Lift (UHL) blades have been introduced. For those profiles, the adverse pressure gradient on the suction side is stronger, resulting in a potential increase of the size of the separation bubble. For multistage components, this problem has been avoided by taking benefit of the wake interactions.

Hence, the design of a modern low-pressure turbine seems to be a challenging task. The designers require reliable tools to simulate and to understand the complexity of the flow over the blades, and especially the transitional flows. Some Computational Fluid Dynamic (CFD) methods are able to simulate very accurately transition. For instance, the Direct Navier-Stokes Simulation (DNS) or the Large Eddy Simulation (LES) provided good results in some cases^{6,7}. However, in an industrial context, where the computational resource is limited and the involved geometries are complex, only the Reynolds Averaged Navier-Stokes Equations (RANS) technique seems appropriate. Thus, transition models have been developed and coupled with RANS turbulence models for industrial uses.

Even if some physical concepts have been developed to model transitional flows⁸, many current models rely on experimental correlations⁹. These correlations are used in a RANS framework through an intermittency function. The value of the intermittency can be obtained from non-local values (for instance depending on integral values of the boundary layer) or from local values.

The aim of this paper is to present how transitional flows can be simulated to meet industrial requirements and constraints. Two transition models using an intermittency function have been implemented into the CFD code TRACE, developed by the German Aerospace Center (DLR). The first model is an in-house model denoted as Multimode^{10,16}. The second model is the $\gamma-Re_{\Theta}$ from Menter *et al*¹¹ with the closure correlations described by Malan *et al*¹³. Those two models will be compared on three different test-cases: the low-pressure turbine cascade profile T106A, the UHL low-pressure turbine cascade profile T106C and a multistage low-pressure turbine named MTU-B⁵.

2 COMPUTATIONAL ENVIRONMENT

The CFD code TRACE code was used for this work. This is a density-based Navier-Stokes solver, developed for special turbomachinery use by DLR¹⁵. All of the transition models are coupled with the k- ω model from Wilcox¹⁴.

2.1 The Multimode Model

This model is an algebraic model which uses non-local values. These values are obtained for structured mesh via an integration over the boundary layer in the direction normal

to the wall. For each transition mode, a value of the intermittency is computed with the help of experimental correlations and of non-local boundary layer values. For the selected transition mode, the intermittency is related to the k - ω turbulence model accordingly to the following equations:

$$\begin{aligned} \frac{\partial(\rho k)}{\partial t} + \frac{\partial(\rho U_i k)}{\partial x_i} &= \gamma \left(\tau_{ij} \frac{\partial U_i}{\partial x_i} - \beta^* \rho k \omega \right) + \frac{\partial}{\partial x_i} \left[(\mu + \sigma_k \mu_T) \frac{\partial k}{\partial x_i} \right] \quad (1) \\ \frac{\partial(\rho \omega)}{\partial t} + \frac{\partial(\rho U_i \omega)}{\partial x_i} &= \max(\gamma, 0.02) \left(\alpha \frac{\omega}{k} \tau_{ij} \frac{\partial U_i}{\partial x_i} - \beta \rho \omega^2 \right) + \frac{\partial}{\partial x_i} \left[(\mu + \sigma_\omega \mu_T) \frac{\partial \omega}{\partial x_i} \right] \end{aligned}$$

The transition model influences the production and the destruction terms in the two equations of the turbulence model. By this mean, the computed boundary layer is indirectly influenced. The source term into the ω -equation is multiplied by at least 0.02. It ensures that a turbulent dissipation is also present inside a laminar boundary layer.

A laminar boundary layer has an intermittency equal to 0 and a fully turbulent boundary layer has an intermittency value of 1. In the case of a separation-induced transition, the intermittency is allowed to grow up to a value of 4. This maximum of 4 remedies the shortcomings of the two equations turbulent model. The turbulence model cannot reproduce the reattachment very well due to the isotropic modelling assumption. Hence, the separated shear layer may reattach and the final value of the intermittency is set to 1. A more complete description of the model has been done by Kožulović¹⁶ and Kožulović *et al*¹⁰.

2.2 The $\gamma - Re_\Theta$ Model

This model has been developed by Menter and Langtry, and has been published in many publications^{11,12,13}. It uses two transport equations: a transport equation for the intermittency γ (2) and a transport equation for the Reynolds number based on the momentum thickness $\tilde{Re}_{\Theta t}$ (3).

$$\frac{\partial(\rho \gamma)}{\partial t} + \frac{\partial(\rho U_i \gamma)}{\partial x_i} = P_\gamma - E_\gamma + \frac{\partial}{\partial x_i} \left[\left(\mu + \frac{\mu_t}{\sigma_f} \right) \frac{\partial \gamma}{\partial x_i} \right] \quad (2)$$

$$\frac{\partial(\rho \tilde{Re}_{\Theta t})}{\partial t} + \frac{\partial(\rho U_i \tilde{Re}_{\Theta t})}{\partial x_i} = P_{\Theta t} + \frac{\partial}{\partial x_i} \left[\sigma_{\Theta t} (\mu + \mu_t) \frac{\partial \tilde{Re}_{\Theta t}}{\partial x_i} \right] \quad (3)$$

$$P_\gamma = f(F_{length}, F_{onset}) \quad (4)$$

$$E_\gamma = f(F_{length}, F_{onset})$$

$$P_{\Theta t} = f(Re_{\Theta t})$$

The parameter F_{onset} controls the start of the transition, while F_{length} influences its length. $Re_{\Theta t}$ is an actual value of the momentum based thickness Reynolds number depending on the boundary layer. In the original publication¹¹, all of the experimental

correlations describing F_{onset} have been published. The authors correlations governing the evolution of Re_{Θ_t} and F_{length} were published later¹². In the meantime, several correlations were published by others authors^{13,17}. The closure correlations implemented in TRACE are those published by Malan *et al*¹³.

According to their authors¹¹, this model is able to simulate all of the transition modes. In addition, the model is also able to simulate the re-laminarisation of a turbulent boundary layer, which happen in the presence of a strong favorable pressure gradient. The value of γ is used for the coupling with the k- ω model as described in Malan *et al*¹³.

Contrary to the multimode model, the intermittency is only used in the k-equation, while the ω -equation remains unchanged. In this case, the maximum value of the intermittency is 2, for the same reasons as in the multimode model.

3 TESTCASES

Three computational testcases will be presented to evaluate the capacity of the models to predict accurately transitional flows. Two testcases are low-pressure turbine cascades: the T106A and the T106C. The last testcase is a five stage low-pressure turbine.

3.1 The T106A Turbine Cascade

The T106A is a low-pressure turbine cascade designed by MTU Aero Engines. It has been extensively investigated in experimental and computational studies. The experimental measurements used for comparison with the computations have been done at DLR Braunschweig¹⁸. The characteristics of the turbine cascade are summarized in the table 1.

inlet angle	-37.7 [°]
outlet angle	30.7 [°]
chord	0.1 [m]
pitch	0.0799 [m]
pitch to chord ratio	0.799 [-]

Table 1: Geometrical parameters of the T106A cascade

The mesh used for the computations, shown in figure 1, is a quasi 3D mesh. It is divided into 8 blocks, for an overall number of points of 19290. In figure 1, every other point is displayed. During all the computations, the first cells in the boundary layer had a value of y^+ lower than one and the boundary layer is resolved with 35 points in the direction normal to the wall.

The performance of the two transition models will be compared with experimental data and also with a fully turbulent computation. All computations were performed accordingly to the flow conditions summarized in table 2.

The results of those computations will be compared in term of pressure coefficient distribution over the blade. In order to asses the capability of the transtions models, the

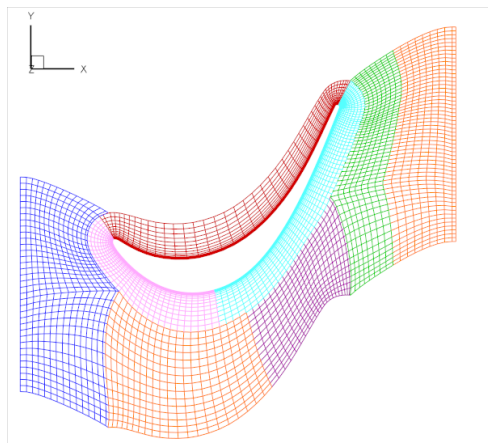


Figure 1: The T106A Mesh

Reynolds Number Re_{2th}	1,5/3/5/7/9/11 [10^5]
inlet angle	-37.7 [°]
Mach Number Ma_{2th}	0.59 [-]
Turbulence Intensity	4 [%]

Table 2: Flow parameters used for the T106A cascade

results of fully turbulent computations and experimental results are also plotted for all Reynolds number in figures 2 and 3.

For the lowest values of the Reynolds number (e.g. 150 000, 300 000 and 500 000, shown in figure 2) a separation bubble can be noticed. The length of the separation bubble is accurately predicted for both transition models. In the region of the separation bubble, the $\gamma - Re_\Theta$ model predicts a pressure coefficient value slightly higher than the one predicted by the multimode model and the one measured during the experiment.

The results for the highest values of the Reynolds number (e.g. 700 000, 900 000 and 1 100 000) are shown in figure 3. In those cases, the boundary layer is turbulent. Then, all the curves are superimposed. The transition model does not have any effect on the development of the boundary layer. This is an important feature for a transition model: it may not impact the accuracy of the turbulence simulation at high Reynolds number. The comparison with the experimental and fully turbulent values is in all cases very good.

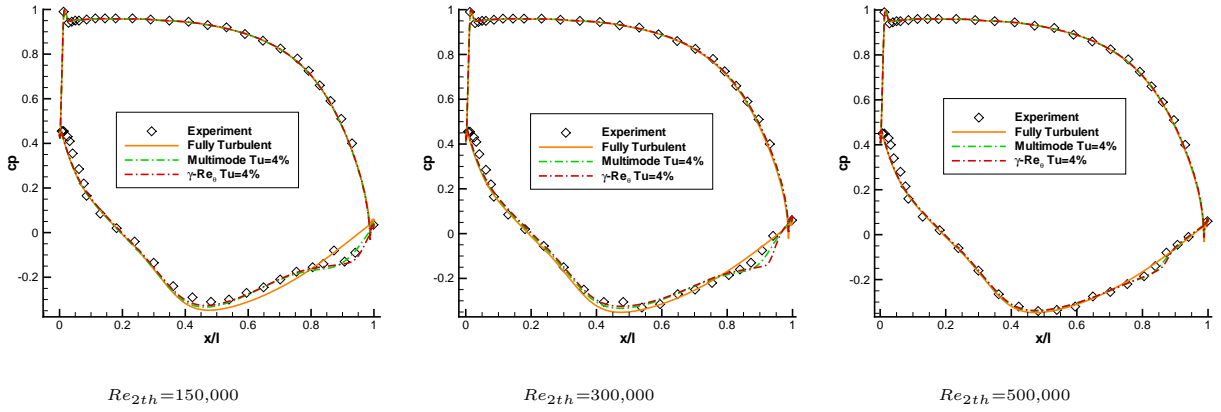


Figure 2: Pressure coefficient distribution over the T106A (Part1)

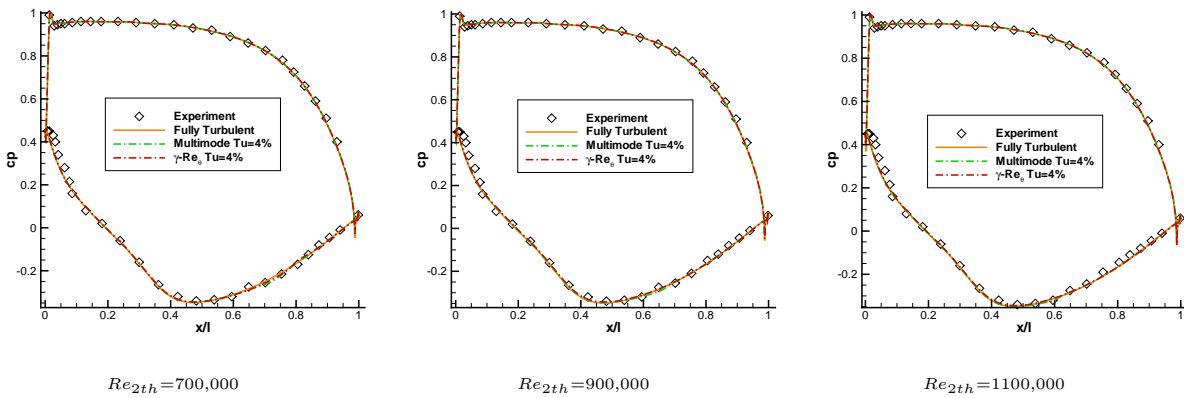


Figure 3: Pressure coefficient distribution over the T106A (Part2)

3.2 The T106C Turbine Cascade

The T106C is also a low-pressure turbine cascade. It has the same profile as the the T106A but the pitch to chord ratio is about 19% higher. The aerodynamic load is then increased, so the expected separation bubble on the suction side would be larger and thicker.

The measurements used here have been performed within the framework of the European Community project TaTMo (Transition and Turbulence Modelling) at the Von Kármán Institute¹⁹.

The characteristics of the turbine cascade are summarized in table 3.

inlet angle	-37.7 [°]
outlet angle	30.7 [°]
chord	0.1 [m]
pitch	0.095 [m]
pitch to chord ratio	0.95 [-]

Table 3: Geometrical parameters of the T106C cascade

The mesh used for the computation of the T106C is shown in the figure 4 (every other point displayed). This is a quasi 3D periodic mesh, divided in 10 blocks. The overall number of points is 26248 and about 30 points are used in the normal direction to the wall to resolve the boundary layer. In all computations, the y^+ value of the first cells is below one.

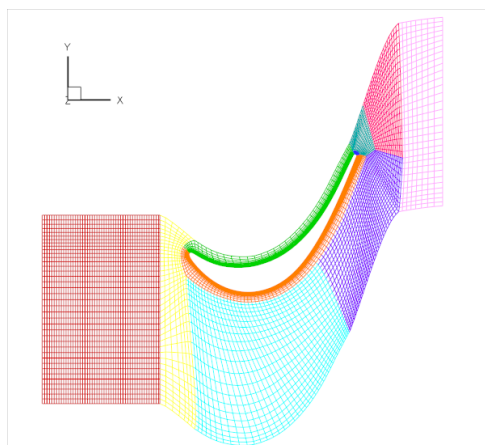


Figure 4: The T106C Mesh

The simulations have been done for different Reynolds numbers while all others parameters remained constant. A summary of the parameters is given in table 4. The results of these computations compared with the experiment are summarized in the Reynolds number lapse rate in figure 5. The Reynolds number lapse rate describes the evolution of

the losses with the Reynolds number. The losses are defined the following way:

$$Losses = 1 - \frac{1 - \left(\frac{P_2}{P_{02}}\right)^{\frac{\gamma-1}{\gamma}}}{1 - \left(\frac{P_2}{P_{01}}\right)^{\frac{\gamma-1}{\gamma}}} \quad (5)$$

where P_{01} is the inlet total pressure, P_{02} is the total pressure at outlet and P_2 is the static pressure at outlet.

Reynolds Number Re_{2th}	1.2/1.4/1.6/1.85/2.1/2.5 [10^5]
inlet angle	-37.7 [°]
Mach Number Ma_{2th}	0.65 [-]
Turbulence Intensity	1 [%]

Table 4: Flow parameters used for the T106C cascade

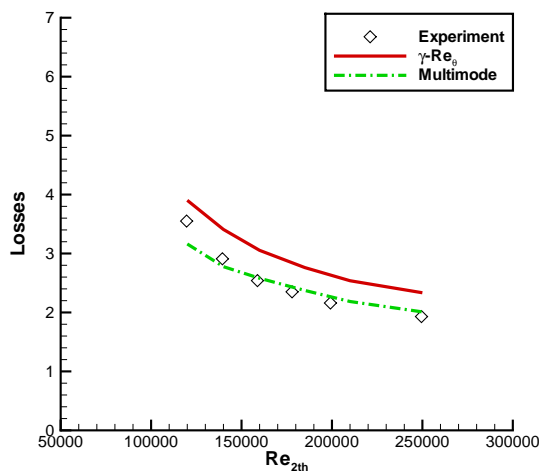
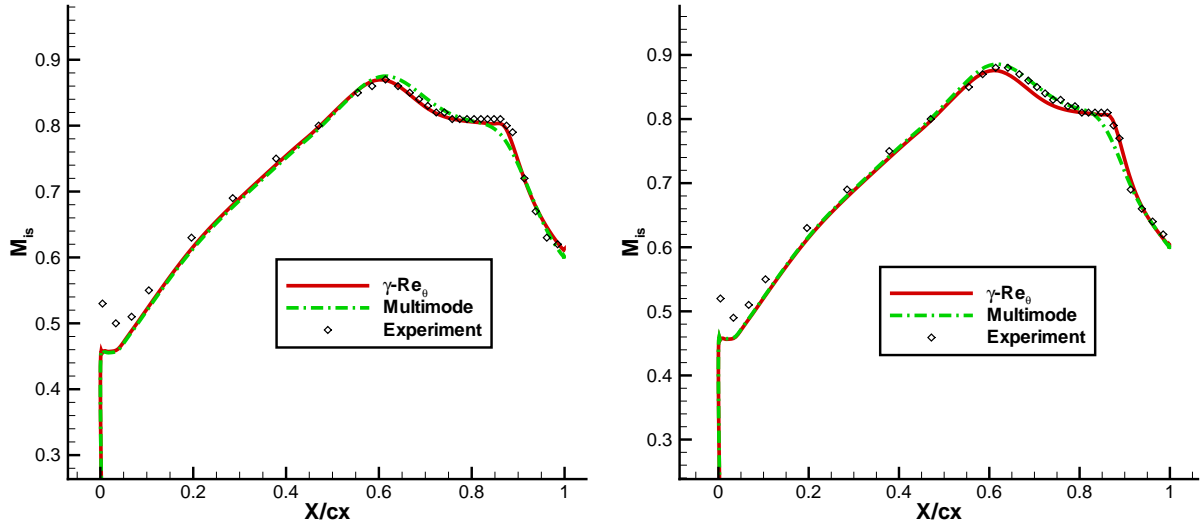


Figure 5: Reynolds Number Lapse Rate of the T106C

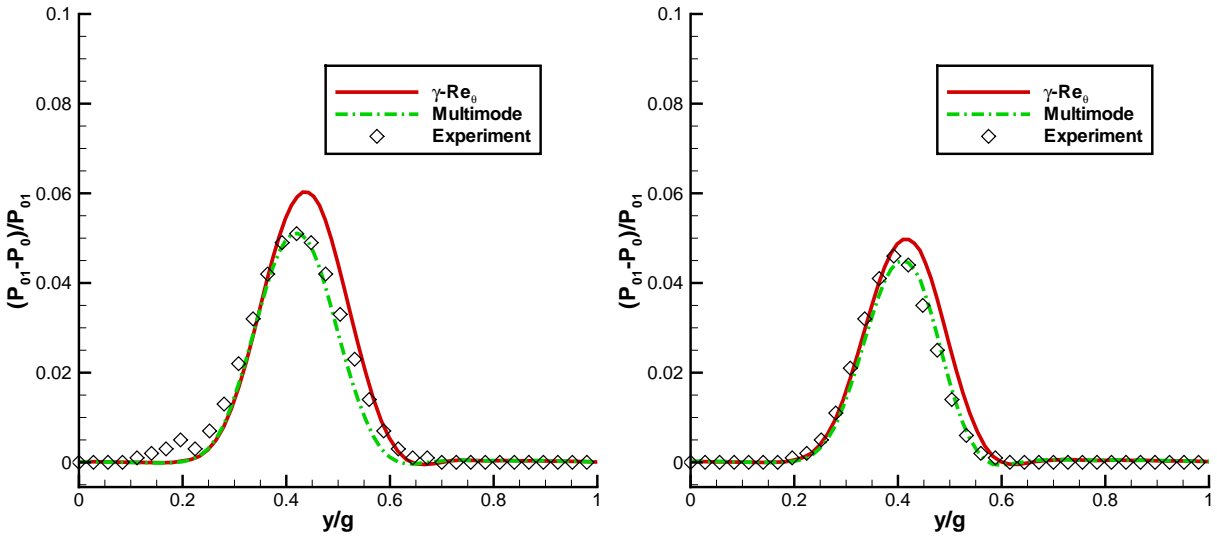
For both models, the curve of the computed losses match the trend of the experimental curve. However, the multimode model values are much closer to the experimental values than the values computed with the $\gamma - Re_{\theta}$ model. In the latest case, the losses are always overestimated. A closer look to the isentropic Mach number distributions and to the wake profile for different Reynolds numbers could help to explain these results. In figure 6, the $\gamma - Re_{\theta}$ model seems to predict a more accurate isentropic Mach number distribution than the Multimode model, and especially the pressure plateau is better described for all Reynolds numbers. Nevertheless, the wake profiles provide an explanation for the overestimated losses. The multimode model is able to simulate a wake very close to the



$Re_{2th} = 120,000$

$Re_{2th} = 160,000$

Figure 6: Isentropic Mach number distribution over the T106C



$Re_{2th} = 120,000$

$Re_{2th} = 160,000$

Figure 7: Wake profiles of the T106C

experimental measurements, because it has been calibrated to work with the $k-\omega$ model implemented in TRACE (see section 2). The wake profiles simulated by the $\gamma-Re_\theta$ model are systematically brighter and deeper. It can be explained by the fact that this model has been originally built and calibrated to work with the $k-\omega$ SST turbulence model¹¹.

3.3 The Multistage MTU-B low-pressure Turbine

The multistage low pressure turbine presented in this paper has been previously presented as MTU-B⁵. This is a five stage turbine, which has been experimentally investigated at the test facility of the University of Stuttgart. The geometry of the turbine is shown in figure 8.

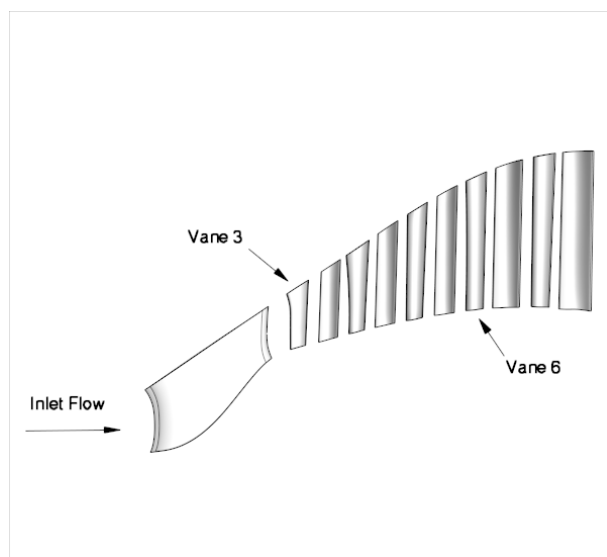


Figure 8: “MTU-B” testcase geometry (side view)

The computations have been performed for different values of the Reynolds number. The isentropic efficiency η_{is} is plotted for each transition model and for the experiment versus the Reynolds number in figure 9. This Reynolds number is defined accordingly to the exit conditions⁵.

The results obtained from both of the transition models are consistent with the experiment. They show a decrease of the efficiency of the MTU-B turbine when the Reynolds number decreases. In addition, it is remarkable to notice that the $\gamma-Re_\theta$ model seems to predict more accurately this evolution.

The pressure coefficient distribution along the blades can provide a good indication on how well is the transition process simulated. Many blades have been instrumented during the experiment. Two blades far from each other could present two different behavior, due to two different flow conditions. Hence the vanes 3 and 6 were chosen to describe the results. The pressure coefficient distributions for each blade are showed at three

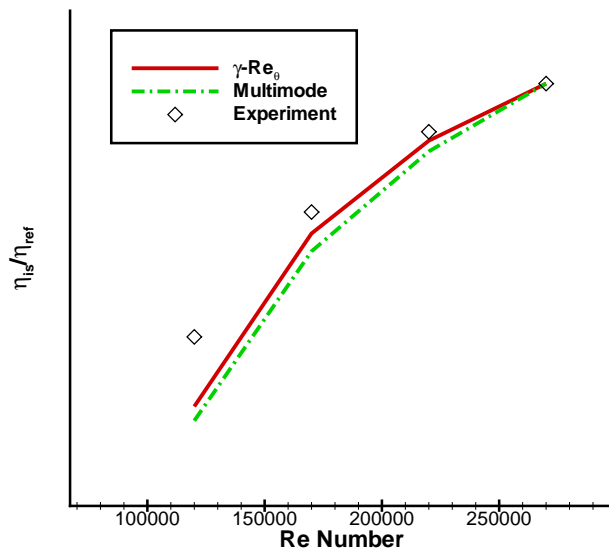


Figure 9: Reynolds laspse rate of MTU-B testcase for different transition models

height of the blade. Along the different rows, the Reynolds number decreases, due to the progressive expansion of the flow in the turbine. In the first row, we could expect that the only transition mode present would be the separation-induced mode. For all of the following rows, this is not so clear. The adverse pressure gradient is present on the suction side of the blades, but the wakes generated by the upstream rows change the free stream turbulence intensity. It then is possible for the bypass mode and the wake-induced mode to be responsible for the transition in the real machine. The situation concerning the transition on those blades is very complex.

In a steady multistage simulation, we cannot simulate a wake-induced transition directly. At the mixing plane, the turbulent kinetic energy is mixed out which leads to a higher turbulent intensity for the inlet of the downstream rows. In the averaged flow field, the $\gamma-Re_\theta$ model describes the effect of wake-induced transition by the bypass mode, which seems to work quite well.

The pressure distribution for vane 3 is shown in figure 10. The pressure coefficient distributions are close for the two models. At 20 percent and 50 percent of the blade height, the separation bubble is quite well simulated by both models, even if the pressure distribution computed with the $\gamma-Re_\theta$ is slightly higher in the region of the separation bubble. At 80 percent of the blade height, it is not clear if the $\gamma-Re_\theta$ model simulate a separation bubble or if this separation bubble is too long. But all in all, the results are satisfactory. The same results for the vane 6 are showed in figure 11.

The aerodynamic load of vane 6 is very high, and we can see that a separation bubble appears over the whole vane. At 20 percent of the blade height, the separation bubble is

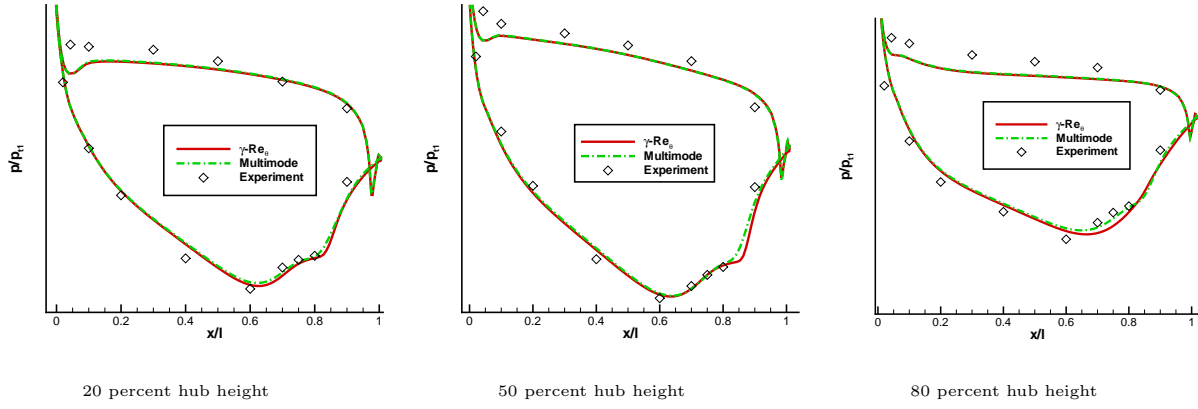


Figure 10: Pressure coefficient distribution over the MTU-B vane 3

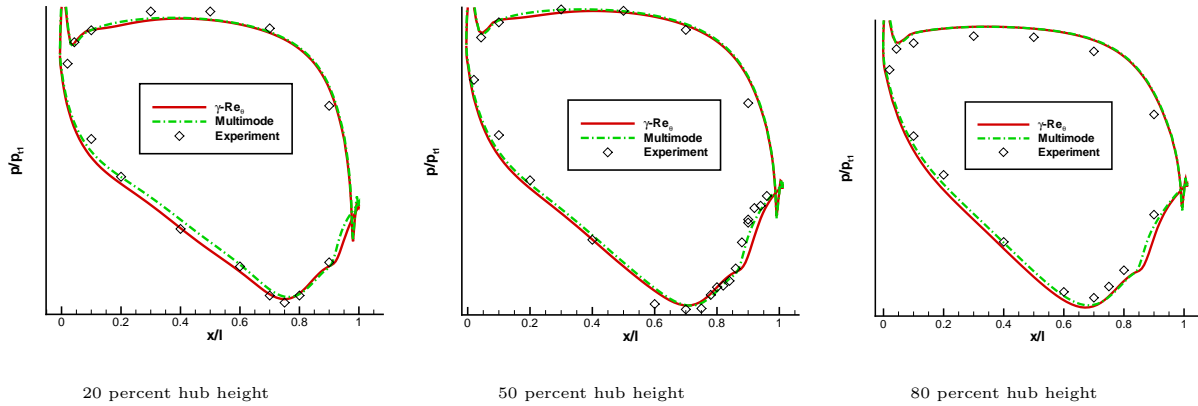


Figure 11: Pressure coefficient distribution over the MTU-B vane 6

quite small and is well reproduced by both models. At midspan and at 80 percent of the blade height, the separation bubble there is longer than the separation bubble predicted at 20 percent blade height. Both models are able to simulate a correct length for the separation bubble.

4 CONCLUSION

This paper described the simulation of transitional flows in industrial context. Especially, the case of the low-pressure turbine was considered. Two transition models were presented. Both of them used experimental correlations, but not in the same frame. The multimode model uses non-local values (hence performs integration over the boundary layer). The γ - Re_{θ} model, using transport equations, works with local variables. Computations using those models were performed and compared with available experimental data on three different test cases: T106A, T106C and a five stage turbine MTU-B.

The two models seemed adequate to simulate all of the different transition modes, even if sometimes the losses were overestimated in the case of the γ - Re_{θ} model. It probably means that the model needs to be tuned to work more accurately in TRACE.

5 ACKNOWLEDGMENTS

A part of the results reported in this paper have been done within the European Commission research project TATMo (contract No. AST5-CT-2006-030939, www.tatmo.eu). The authors would like to thank the partners in European Union FP6 programm TATMo for permitting the publications of the results in this paper. In addition, the authors would like to thank also MTU Aero Engines, for the permission to publish the results about the MTU-B Multistage Turbine.

REFERENCES

- [1] Hermann Schlichting, Boundary Layer Theory, Seventh Edition, *McGraw Hill*.
- [2] Mayle, R. E., The role of laminar-turbulent transition in gas turbines engines, *ASME J. Turbomachinery*, **113**, 509–537 (1991).
- [3] Frank M. White, Viscous Fluid Flow, Second Edition, *McGraw Hill*.
- [4] Hatman, A., Wang, T., A Prediction Model for Separated-Flow Transition, *ASME J. Turbomachinery*, **121**, 594–602 (1999).
- [5] Gier, J., Franke, M., Hübner, N. and Schröder, T., Designing LP Turbines for Optimized Airfoil Lift, *ASME Paper*, GT2008-51101 (2008).
- [6] Wissink, J. G., Rodi, W., Direct Numerical Simulations of Transitional Flow in Turbomachinery, *ASME J. Turbomachinery*, **128**, 668–678 (2006).

- [7] Lardeau, S., Li, N., Leschziner, M. A., Large Eddy Simulation of Boundary Layers at High Free-Stream Turbulence Intensity and Implications for RANS Modeling, *ASME J. Turbomachinery*, **129**, 311–317 (2007).
- [8] Mayle, R. E., Schulz, A., The Path to Predicting Bypass Transition, *ASME J. Turbomachinery*, **119**, 405–411 (1997).
- [9] Abu-Ghannam, B. J., Shaw, R., Natural transition of boundary layers - The effects of turbulence, pressure gradient and flow history, *J. Mechanical Engineering Science*, **22-5**, 213–228 (1980).
- [10] Kožulović, D., Röber, T., Nürnberger, D., Application of a Multimode Transition Model to Turbomachinery Flow, *Proc. of the European Turbomachinery Conference*, (2007).
- [11] Menter, F. R., Langtry, R. B., Völker, S., Transition Modelling for General Purpose CFD Codes, *6th International Symposium on Engineering Turbulence Modelling and Measurements*, Sardinia, Italy (2005).
- [12] Langtry, R. B., Menter, F. R., Correlation-Based Modeling for Unstructured Parallelized Computational Fluid Dynamics Codes, *AIAA Journal* **47-12**, 2894–2906 (December 2009).
- [13] Malan, P., Suluksna, K., Juntasaro, E., Calibrating the γ - Re_{Θ} Transition Model, *ERCFTAC Bulletin 80*, 53–57 (2009).
- [14] Wilcox, D. C., Turbulence Modeling for CFD, Second Edition, *DCW Industries*.
- [15] Kügeler, E., Weber, A., Nürnberger, D. and Engel, K., Influence of Blade Fillets on the Performance of a 15 stage Gas Turbine Compressor, *Proceedings of ASME Turbo Expo 2008: Power for Land, Sea and Air*, GT-50748 (2008).
- [16] Kožulović, D., Modellierung des Grenzschichtumschlags bei Turbomaschinenströmungen unter Berücksichtigung mehrerer Umschlagsarten, *DLR Forschungsbericht 2007-20*, (2007) (*In German*).
- [17] Piotrowski, P., Elsner, W., Drobniak, S., Transition Prediction on Turbine Blade Profile with Intermittency Transport Equation, *Proceedings of ASME Turbo Expo 2008: Power for Land, Sea and Air*, GT2008-50796 (2008).
- [18] Hoheisel, H., Entwicklung neuer Entwurfskonzeptefr zwei Turbinengitter, Teil 3 Ergebnisse T106, *DFLR Bericht*, Braunschweig (1981).

- [19] Michalek, J. and Arts, T., Aerodynamic Performance of a Very High Lift Low Pressure Turbine Airfoil (T106C) at Low Reynolds Number and High Mach Number with Effect of Free Stream Turbulence Intensity and Upstream Passing Wakes *ASME paper* GT2010-22884 (2010).